ICARUS 42, 211–233 (1980)

Effects of Atmospheric Breakup on Crater Field Formation[1]

QUINN R. PASSEY AND H. J. MELOSH[2]

Division of Geological and Planetary Sciences, California Institute of Technology, Pasadena, California 91125

Received October 5, 1979; revised February 18, 1980

This paper investigates the physics of meteoroid breakup in the atmosphere and its implications for the observed features of strewn fields. There are several effects which cause dispersion of the meteoroid fragments: gravity, differential lift of the fragments, bow shock interaction just after breakup, centripetal separation by a rotating meteroid, and possibly a dynamical transverse separation resulting from the crushing deceleration in the atmosphere. Of these, we show that gravity alone can produce the common pattern in which the largest crater occurs at the downrange end of the scatter ellipse. The average lift-to-drag ratio of the tumbling fragments must be less than about 10^{-3}, otherwise small fragments would produce small craters downrange of the main crater, and this is not generally observed. The cross-range dispersion is probably due to the combined effects of bow shock interaction, crushing deceleration, and possibly spinning of the meteoroid. A number of terrestrial strewn fields are discussed in the light of these ideas, which are formulated quantitatively for a range of meteoroid velocities, entry angles, and crushing strengths. It is found that when the crater size exceeds about 1 km, the separation between the fragments upon landing is a fraction of their own diameter, so that the crater formed by such a fragmented meteoroid is almost indistinguishable from that formed by a solid body of the same total mass and velocity.

INTRODUCTION

It has been estimated that over 70,000,000 meteoroids enter the Earth's atmosphere each day. Of these, about 1000 kg (about 1%) of the meteoric material survives the ablative effects of atmospheric descent and strikes the surface (Baldwin, 1963, pp. 6–7).

The meteoroids are subjected to high pressures and stresses while traveling through the atmosphere at velocities of several kilometers per second and often break into fragments which may or may not survive the remaining descent to the surface. The altitude at which breakup occurs generally varies from 4 to 40 km, and appears to be independent of either the mass or class of the meteorite (Krinov, 1960, pp. 76–77).

After breakup, the fragments fall over an area which is roughly elliptical in shape. If the impacting meteorites have sufficient kinetic energy to produce craters, a crater field is created in this same elliptical form and is often referred to as a strewn field or scatter ellipse.

Within this crater field, the individual meteorites, or craters, are distributed in a systematic manner; the largest masses or craters are generally located at, or near, the downrange boundary of the crater field while the smallest masses fall at the uprange boundary. There is also a cross-range distribution of craters which we show can be the result of a transverse velocity supplied to the meteoroid fragments at the time of the interaction of bow shocks coupled with the effects of crushing the meteoroid. Lift can also affect the distribution of craters but we find that it is negligible except for the case of fragments of masses less than about 10^2 kg. Also, some deviations from a regular distribution of craters can be

[1] Contribution No. 3328 of the Division of Geological and Planetary Sciences, California Institute of Technology, Pasadena, Calif. 91125.

[2] Present address: Department of Earth and Space Sciences, SUNY, Stony Brook, N.Y. 11794.

0019-1035/80/050211-23$02.00/0

explained by multiple breakup or relatively steep angles of entry.

This paper is primarily concerned with crater fields but there are several single terrestrial craters which may be the result of the almost simultaneous impacts of meteoroid fragments which, due to the angle of entry or altitude of breakup, were not sufficiently separated from one another to form individual or obviously overlapping craters. Some possible examples of these include: Boxhole Crater, Brent Crater, Dalgaranga Crater, Holleford Crater, Meteor (Barringer) Crater, New Quebec (Chubb) Crater, and Wolf Creek Crater (Baldwin, 1963; Barringer, 1967; Heide, 1963; Krinov, 1960, 1966; Millman, 1971).

We first discuss the principal features of several well-known terrestrial strewn fields, illustrated by maps of the fields, and establish a measure of the crater dispersion in these fields. We then review the physics of atmospheric entry and summarize our computational scheme. We study the effects of gravity, lift, bow shock interaction, spinning meteoroids, and crushing deceleration within the context of this model. The theory is then applied to the observed crater fields and it is concluded that gravity, bow shock interactions, and possibly spinning play the major roles in strewn field formation with the effects of crushing deceleration and lift playing minor roles. Theoretical plots are constructed showing the fate of meteoroids of given masses, velocities, yield strengths, and angles of entry into earth's atmosphere. It is found that strewn fields are important only for craters less than about 1 km in diameter; in the case of larger craters, the fragments fall so close together (for entry angles greater than approximately 10°) that the crater is almost indistinguishable from that made by a single solid meteoroid.

TERRESTRIAL CRATER FIELDS

Explanation

No field study for any crater field discussed in this paper was undertaken. Rather, the information is based entirely upon publications.

The diameters of the craters listed in this paper are generally from the measurements by previous authors. However, a few of the diameters listed herein were estimated from published maps of the crater fields. The diameters refer to the present rim-to-rim crater diameter without respect to a reconstructed crater diameter and is probably somewhat smaller than the original rim-to-rim diameter due to erosion of the rim.

The distances recorded in the tables were derived from maps or from written descriptions as supplied by previous authors, and represent the distance from the center of the crater in question to the center of the largest crater of the field. The largest crater is used as the origin of coordinates because it usually marks the distant end of the scatter ellipse. Where the largest crater does not lie near one end of the field (as with the Campo del Cielo crater field) no distances are listed.

Campo del Cielo

The Campo del Cielo crater field is located within the Chaco and Santiago del Estero Provinces, Argentina (27°38′S, 61°42′W), and is composed of at least 20 craters (Romaña and Cassidy, 1973). The distribution of craters is along a line trending SW–NE, with the largest crater in the middle, rather than at one end, of the crater field (Cassidy *et al.*, 1965) (refer to Table I).

It has been suggested that the impact angle for the meteorite involved in the formation of crater 9 was about 22° and that the final impact velocity was not greater than 5.8 km sec^{-1} (Cassidy and Renard, 1970; Cassidy, 1971; Renard and Cassidy, 1971).

Meteorites found in the immediate area are composed of iron (hexahedrite class) and samples have been recovered ranging in mass from 50 g to 4210 kg (Milton, 1963). Studies have also revealed a meteorite with an estimated mass of 22,000 kg in crater 10

TABLE I

CAMPO DEL CIELO[a]

Crater number	Crater diameter[b] (m)	Distance from largest crater[c] (m)
1	85	NA[d]
2	71	NA
3	103	NA
4	89	NA
5	45[e]	NA
6a	35	NA
6b	20	NA
7	85	NA
8	37	NA
9	40	NA
10	22[f]	NA
11–20	Not given	NA

[a] Data from Cassidy and Renard (1970), Cassidy (1971), Romaña and Cassidy (1973), Cassidy *et al.* (1975).
[b] Average rim-to-rim diameter.
[c] Center-to-center.
[d] Not applicable (reference point is uncertain since the largest crater is not near the downrange end of the crater field).
[e] Average floor diameter.
[f] Average reconstructed diameter.

(Cassidy, 1970, 1978 personal communication).

Clearwater Lakes

In northern Quebec (56°N, 74 ½°W) are two nearly circular lakes with diameters of 32 and 26 km. These are known as Clearwater Lakes and the center-to-center separation is approximately 31 km. A geologic study of these basins by Kranck and Sinclair (1963) suggested that they were of volcanic–tectonic origin. Other studies, however, state that these two basins are of meteorite-impact origin (Beals *et al.*, 1956; Beals *et al.*, 1960; Irwin, 1963; Dence *et al.*, 1977).

Henbury

The crater field near Henbury cattle station in central Australia (24°35′S, 133°10′E) is composed of at least 15 separate or overlapping craters (Milton, 1968) (refer to Fig. 1 and Table II).

This crater field is one of the best preserved examples of a scatter ellipse. The direction of the impact is inferred to have been from the SW to the NE, as evidenced by the location of the largest craters with respect to the smaller craters.

Meteoritic iron (octahedrite class) has been found at the site (Hodge, 1965; Krinov, 1966) and the largest meteorite recovered has a mass of about 150 kg (Baldwin, 1963).

Herault

The Herault craters are located in southern France (43°30′N, 3°15′E) near the towns of Faugères and Cabrerolles (Beals, 1964; Gèze and Cailleux, 1950; Janssen, 1951; Hoffleit, 1952).

In studying the crater profiles, Beals states that there is a possibility that the craters are not of meteoritic origin because none of them exhibited a raised rim. If,

TABLE II

HENBURY[a]

Crater number[b]	Crater diameter[c] (m)	Distance from largest crater[d] (m)
1	147	—
2	119	55
3	79	122
4	54	143
5	47	393
6	42	323
7	24	381
8	24	500
9	23	422
10	20	463
11	20 (?)	204
12	20	291
13	14	441
14	9	579
15	8	467
16	7 (?)	626

[a] Data from Milton (1968); Hodge (1965).
[b] This paper only.
[c] Average rim-to-rim diameter.
[d] Center-to-center.

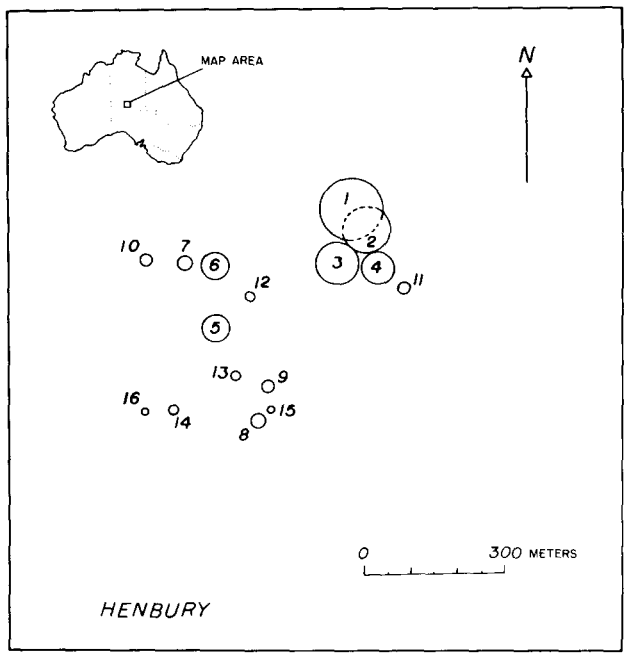

FIG. 1. Schematic map of the Henbury crater field in Australia (modified from Milton, 1968; Hodge, 1965).

however, the craters are the products of a fragmented meteoroid, the trajectory appears to have been from the NE to SW (refer to Fig. 2 and Table III).

Kaalijarv

On the Baltic island of Oesel, Estonia (58°24'N, 22°40'E) lies a group of nine craters which are known as the Kaalijarv craters. The largest crater (Gut Sall) is located at one end of the field and the inferred trajectory is from SSW to NNE (refer to Fig. 3 and Table IV) (Kraus *et al.*, 1928; Heide, 1963; Krinov, 1966).

Small fragments of meteoritic iron (octahedrite class) have been found associated with the craters (Krinov, 1961; Baldwin, 1963).

Lonar

Lonar crater lies in the Deccan Plateau region of India (19°58'N, 76°31'E). It is presently occupied by a shallow alkaline lake 1830 m in diameter. A second crater which is 300 m in diameter is located approximately 700 m north of the rim of the main crater (center-to-center distance about 1300 m) (Fredriksson *et al.*, 1973).

The origin of Lonar Lake was considered to be volcanic by some authors (Nandy and Deo, 1961; Heide, 1963), while later investi-

TABLE III

HERAULT[a]

Crater number[b]	Crater diameter[c] (m)	Distance from largest crater[d] (km)
1	200	—
2	72	5.4
3	57	5.6
4	55[e]	6.8[f]
5	48	6.8
6	15	7.1

[a] Data from Geze and Cailleux (1950), Janssen (1951), Hoffleit (1952).
[b] This paper only.
[c] Average rim-to-diameter.
[d] Center-to-center, ±0.2 km.
[e] ±7 m.
[f] ±0.5 km.

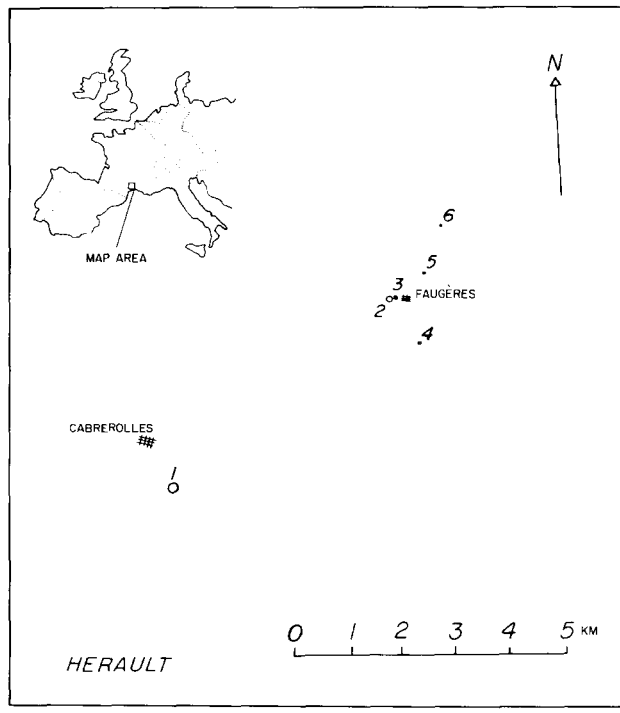

FIG. 2. Schematic map of the Herault, France, crater field. Note: the locations of the craters are only approximate because they were plotted from written descriptions with respect to the towns of Cabrerolles and Faugères (Gèze and Cailleux, 1950; Janssen, 1951; Hoffleit, 1952).

gations have revealed samples of rock that have been shock metamorphosed and meteoritic origin is now proposed (Lafond and Dietz, 1964; Fredriksson *et al.*, 1973). An ejecta blanket associated with the main crater has also been described (Milton and Dube, 1977).

TABLE IV

KAALIJARV[a]

Crater number[b]	Crater diameter[c] (m)	Distance from largest crater[d] (m)
1	110	—
2	44	758
3	35	342
4	33[e]	942
5	26[e]	447
6	20	374
7	20	621
8	14[e]	442
9	4.5	884

[a] Data from Krinov (1966).
[b] This paper only.
[c] Rim-to-rim.
[d] Center-to-center.
[e] Average from elongated crater.

Mauritanian Craters

Three craters of, presumably, meteoritic origin are located in Mauritania in western Africa. The southernmost crater, Aouelloul (20°15'N, 12°41'W) has a diameter of about 380 m. The largest crater, Tenoumer (22°55'N, 10°24'W), has a diameter of 1920 m, and the northernmost crater, Temimichat Ghallaman (24°15'N, 9°39'W) is about 700 m in diameter. The separation between Aouelloul and Temimichat Ghallaman is approximately 600 km.

Meteoritic iron has been found associated with Aouelloul (Krinov, 1966) as well as the presence of glassy fragments (Fudali and Cassidy, 1972). The evidence for impact origin of Tenoumer includes: shock

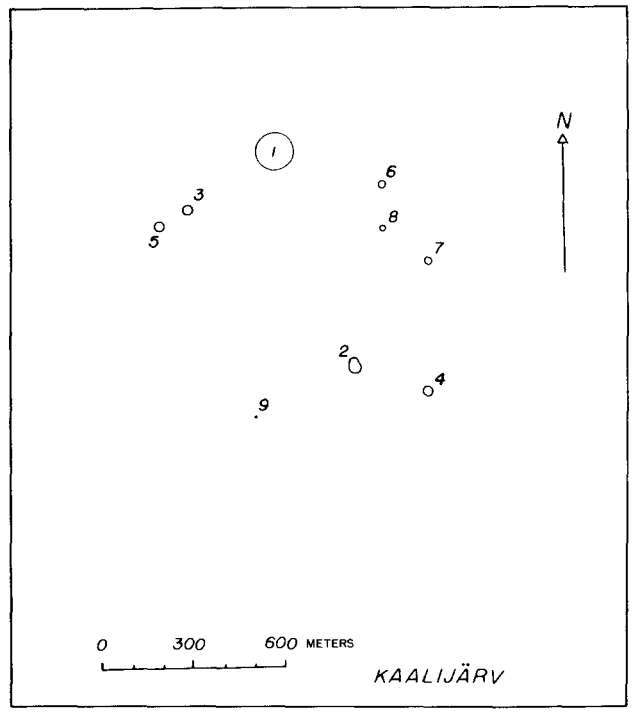

FIG. 3. Schematic map of Kaalijarv crater field (after Krinov, 1966).

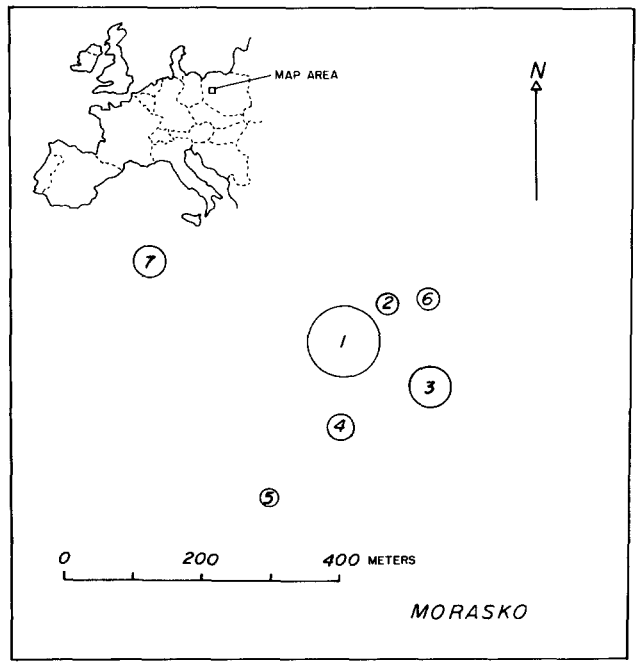

FIG. 4. Schematic map of the Morasko crater field (modified from Korpikiewics, 1978).

TABLE V

MORASKO[a]

Crater number	Crater diameter (m)	Distance from largest crater[b] (m)
1	100	—
2	25	86
3	63	139
4	35	123
5	15	255
6	24	136
7	50	305
8	35	NA[c]

[a] Data from Korpikiewicz (1978).
[b] Center-to-center.
[c] Not available.

lamellae in quartz, mineralogical transformations, and occurrence of lechatelierite, apparently derived from highly shocked quartz. As of 1972 (Fudali and Cassidy, 1972), there was no petrographic evidence for an impact origin of Temimichat Ghallaman.

The three craters have an almost perfect alignment trending N35°E and it has been suggested (Fudali and Cressy, 1976) that they represent a simultaneous triple impact of a fragmented meteoroid traveling a very shallow atmospheric trajectory.

Morasko

North of Poznan, Poland, near the village of Morasko (52°30'N, 16°55'E) lies a group of eight craters. The largest crater is 100 m in diameter with a depth of 13 m (refer to Fig. 4 and Table V).

Iron meteorites (octahedrite class) have been recovered in the area and it has been estimated that the direction of the trajectory was from SSW to NNE (Classen, 1978; Korpikiewicz, 1978; *Sky & Tel.* 1979).

Odessa

The Odessa crater field, in west-central Texas (31°43'N, 102°25'W) consists of five craters (refer to Fig. 5 and Table VI).

Abundant iron fragments (octahedrite class) have been recovered from this area (Evans, 1961; Krinov, 1966). Baldwin (1963) calculates that the main impacting

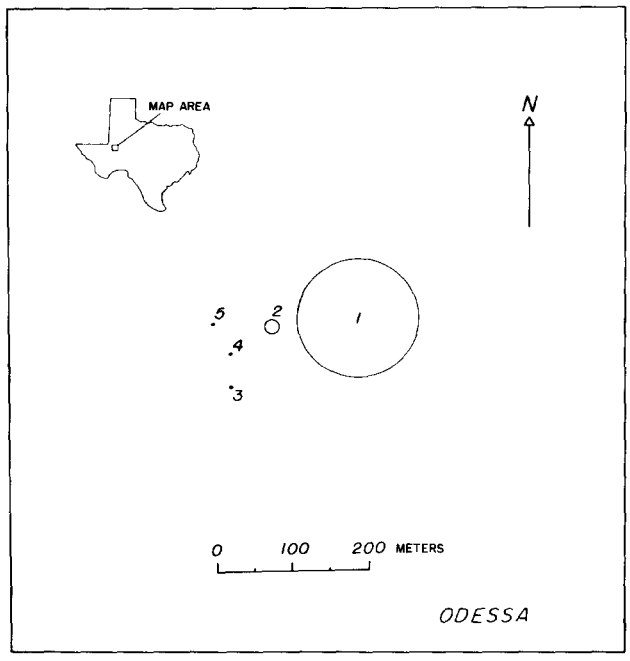

FIG. 5. Schematic map of the Odessa crater field, Texas (after Evans, 1961).

TABLE VI

ODESSA[a]

Crater number[b]	Crater diameter[c] (m)	Distance from largest crater[d] (m)
1	168	—
2	21	119
3	10	200
4	8 (?)	182
5	6	200

[a] Data from Evans (1961).
[b] This paper only.
[c] Rim-to-rim, ±5 m.
[d] Center-to-center.

meteorite had a mass of about 315 tons and was accompanied by at least four smaller meteoroids at the time it entered the atmosphere. It is more likely that a single meteoroid entered the atmosphere and that the fragments producing the smaller craters were a result of fragmentation which occurred during its fall to the surface.

The trajectory has an eastward component, as indicated by a cross section of crater 2 (Evans, 1961) and this corresponds with the direction inferred by the relative positions of the craters of from WSW to ENE.

Sikhote-Alin

The Sikhote-Alin crater field is located in Siberia, USSR (46°6′N, 134°42′E). Over 150 craters ranging in diameter from 26.5 to about 0.1 m are associated with this fall as well as thousands of meteoritic fragments. The fall occurred on February 12, 1947, and because of its recent nature, many small craters were recorded which are not observed associated with much older crater fields. Refer to Krinov (1966) for a map of the scatter ellipse and crater locations.

The total mass of the fall has been estimated to be about 70 tons (Krinov, 1966, 1974) and it has been estimated that at least 200 tons of meteoritic matter were contained in the smoke trail (Heide, 1963).

Krinov (1974) has developed a qualitative model to describe the presence of secondary scatter ellipses superposed on the main

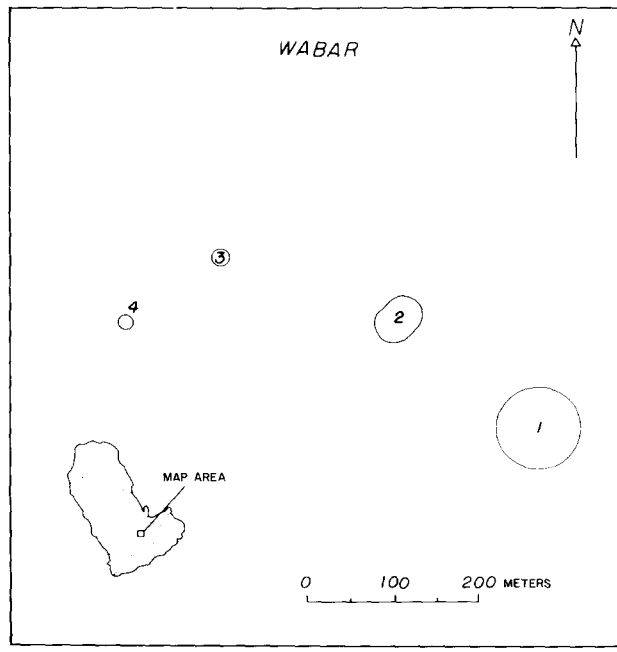

FIG. 6. Schematic map of Wabar crater field (after Philby, 1933).

ellipse. He describes a series of three stages of breakup at different altitudes.

Fesenkov (1951) and Krinov (1966) calculate that the meteoroid entered the Earth's atmosphere with a velocity of 14–15 km sec^{-1} and that a breakup occurred at an altitude of approximately 6 km which probably relates to the third stage of breakup referred to by Krinov (1974).

Wabar

The Wabar crater field is located in the Great South Desert of Arabia (21°29'N, 50°28'E) in the Rub' al Khali. Philby (1933) discovered the craters and various authors (Bartrum, 1932; Baldwin, 1963; Krinov, 1966) state that two craters make up this field. Other authors (Holm, 1962; Heide, 1963) give the number of craters as four or five, respectively (refer to Fig. 6 and Table VII).

Fragments of meteoritic iron (octahedrite class) have been found in the area and a total mass of about 12 kg have been recovered (Krinov, 1966).

The trajectory is believed to have been from WNW to ESE as suggested by the configuration of the craters.

TABLE VII

WABAR[a]

Crater number[b]	Crater diameter[c] (m)	Distance from largest crater[d] (m)
1	100	—
2	55 × 40	207
3	20	421
4	17	498

[a] Data from Philby (1933).
[b] This paper only.
[c] Rim-to-rim, ±5 m.
[d] Center-to-center.

A NUMERICAL MODEL FOR CRATER FIELD FORMATION

PHYSICAL THEORY OF METEORS

Introduction

The fall of a meteorite begins when it enters the upper atmosphere. Its initial geocentric velocity can range from 11.2 to about 70 km sec^{-1} assuming the meteoroid to be in a heliocentric orbit. Its entry angle can also range from near zero to 90° with respect to the local horizontal with 45° being the most likely entry angle (Gilbert, 1893).

As the meteoroid collides with atoms in the air, some of its kinetic energy is dissipated. Some of this energy is used in ablating the body by melting and/or vaporizing the exposed surface. Some of its momentum is also transferred to the air and the resultant atmospheric drag decelerates the meteoroid.

At supersonic velocities, a bow shock is produced and the meteoroid is subjected to high stresses. When these stresses exceed the yield strength of the body, fragmentation occurs. After breakup, the individual fragments decelerate differentially according to their relative masses and gravity causes a vertical separation of the individual trajectories of the fragments. The smaller fragments are decelerated the fastest and are, therefore, the most affected by gravity and fall short of the larger fragments.

Equations

The simplest model for atmospheric entry and trajectory of a meteoroid assumes that the Earth is flat (refer to Fig. 7). For this case the equations governing the motion and ablation of the meteoroid are as follows (Fesenkov, 1951; Thomas and Whipple, 1951; Allen and Eggers, 1958; Baldwin and Sheaffer, 1971; Renard and Cassidy, 1971):

$$\frac{dV}{dt} = -\frac{C_D \rho_a A V^2}{M} + g \sin\theta \qquad (1)$$

$$\frac{dM}{dt} = -\tfrac{1}{2}\frac{C_H \rho_a A V^2}{\zeta}\left(\frac{V^2 - V_{CR}^2}{V^2}\right), \qquad (2)$$

$$\frac{d\theta}{dt} = \frac{Mg\cos\theta - \tfrac{1}{2}C_L \rho_a A V^2}{MV}, \qquad (3)$$

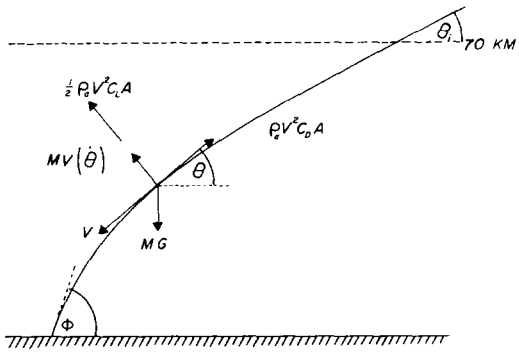

FIG. 7. Schematic diagram of the kinematic forces acting on a meteoroid during flight through the atmosphere. The initial entry of the meteoroid into the atmosphere is assumed to be at 70 km altitude for the calculations presented in this paper.

$$\frac{dZ}{dt} = -V \sin \theta, \tag{4}$$

and

$$\frac{dX}{dt} = V \cos \theta, \tag{5}$$

where

$$\rho_a = \rho_0 \exp(-Z/H) \tag{6}$$

and (Jacchia, 1958; Jacchia *et al.*, 1967)

$$A = S_F(M/\rho_m)^{2/3}. \tag{7}$$

In the above equations, A is the effective cross-sectional area of the meteoroid, M is the mass, S_F is the shape factor, ρ_m is the density of the meteoroid, and ζ is the heat of ablation for the meteoroidal material.

The coefficients for lift and drag are respectively C_L and C_D and the heat transfer coefficient is C_H. The angle θ is with respect to the local horizontal, the meteoroid velocity is V and the critical velocity is V_{CR}. Time is t, acceleration of gravity is g, and downrange distance is X.

The local air density ρ_a is a function of the sea-level density ρ_0, the altitude Z, and the scale height H.

For a spherical planet, Eqs. (3) and (5) must be modified to include terms for the curvature of the planet. The modified equations are (Gazley, 1961):

$$\frac{d\theta}{dt} = \frac{Mg \cos \theta - \frac{1}{2}C_L \rho_a A V^2}{MV} - \frac{V \cos \theta}{R_E + Z}, \tag{8}$$

and

$$\frac{dX}{dt} = \frac{V \cos \theta}{1 + Z/R_E}, \tag{9}$$

where R_E is the radius of the Earth.

CRATER DIAMETERS

Various crater energy-diameter scaling laws have been proposed (Baldwin, 1963; Gault, 1974; Moore, 1976; Dence *et al.*, 1977) which all have the general formula

$$D \sim (E_k)^\gamma,$$

where D is the diameter (in centimeters), E_k is the impacting kinetic energy (ergs), and γ is approximately $\frac{1}{3}$. For this paper, the following energy-diameter scaling equations are used (Gault, 1974):

$$D = 0.0015\ \rho_m^{1/6} \rho_t^{-1/2} (E_k)^{0.37} (\sin \varphi)^{2/3}, \tag{10}$$

$$D = 0.025\ \rho_m^{1/6} \rho_t^{-1/2} (E_k)^{0.29} (\sin \varphi)^{1/3}, \tag{11}$$

$$D = 0.027\ \rho_m^{1/6} \rho_t^{-1/2} (E_k)^{0.28} (\sin \varphi)^{1/3}, \tag{12}$$

where ρ_t is the density of the target material and φ is the impact angle with respect to the horizontal.

The first equation (10) is for impacts against massive rock with resultant craters up to 10 m in diameter. There is a gradual transition to the second equation (11) which is valid up to 100-m diameter craters. The third equation is valid for craters of kilometer dimensions, with a gradual transition between the last two equations between 100- and 1000-m diameter craters.

SPECIFICATIONS FOR NUMERICAL MODELING

Meteor theory contains several unknown parameters which include: shape, heat transfer coefficient, drag coefficient, and lift-to-drag ratio. These parameters, therefore, have to be estimated for numerical modeling.

For simplicity, the calculations assume that the meteoroid is spherical and this is

approximately correct if a nonspherical meteoroid is spinning rapidly as it descends. The shape factor (S_F) for a spherical body is a dimensionless quantity and a value of 1.21 is used (McKinley, 1961, p. 173). The lift-to-drag ratio is assumed to be zero (C_L = 0.0), however, several calculations were made to determine the maximum value that the lift coefficient could have and still produce the distribution of craters found in known crater fields (this is discussed later).

The value of the heat transfer coefficient (C_H), has been suggested to be in the range of 0.6 to 0.1 or less (McKinley, 1961, p. 174). Values of the order 10^{-2} have also been considered. This coefficient is a strong function of speed, altitude, and body size (Allen *et al.*, 1963; Seiff and Tauber, 1966) but for the calculations presented here, a constant value of 0.02 is used. The choice for the value of this parameter is not as important for masses larger than 10^6 kg, as are of interest in this paper, as it is for meteoroid masses 10^4 kg or less (Renard and Cassidy, 1971).

The heat of ablation (ζ) for an iron meteoroid is a combination of the heat of fusion ($\zeta_f = 1.89 \times 10^6$ J kg^{-1}) and the heat of vaporization ($\zeta_v = 8.01 \times 10^6$ J kg^{-1}) (Baldwin and Sheaffer, 1971). The combined value used in this paper is 5.0×10^6 J kg^{-1}.

There exists a velocity below which no appreciable ablation occurs for a given density of air. This is known as the critical velocity (V_{CR}) for which we use a value of 3.0 km sec^{-1}. This is the experimentally determined velocity below which steel pellets do not glow at sea-level air densities (Allen *et al.*, 1952).

The drag coefficient (C_D) for a spherical meteoroid is approximately 0.5, and this value is assumed in the calculations presented in this paper (Hawkins, 1964, pp. 17–18).

Iron meteoroids with a density (ρ_m) of 7.8×10^3 kg m^{-3} are assumed to impact a target with a density (ρ_t) of 3.0×10^3 kg m^{-3} for the calculation of crater diameters.

The scale height (H) for the Earth's atmosphere varies from 6.4 km at high altitudes to 8.4 km at sea level. We assume a constant average value of 7.2 km (Renard and Cassidy, 1971). The numerical calculations begin at an altitude of 70 km. Above this, there is no significant ablation of meteoroids whose masses are greater than about 10^4 kg.

Breakup

The fragmentation process of a meteoroid is not fully understood. The presence of preexisting defects or planes of weakness in the meteoroid can strongly influence its breakup. Some of the mechanisms proposed to cause fracturing include thermomechanical stresses (Lang, 1977) and aerodynamic pressures (Baldwin and Sheaffer, 1971). The latter is treated in this paper because the aerodynamic model for fragmentation dominates the thermomechanical model at altitudes less than 80 km.

The actual mechanics of fragmentation is a process unique to each meteoroid and the number of fragments produced can range from two to large numbers.

Buddhue (1942) sampled iron meteorites from nine separate falls and found that their crushing strengths varied from 6×10^6 to 4×10^8 N m^{-2}. Values of 2×10^5 (Opik, 1958) and 5×10^8 N m^{-2} (Baldwin and Sheaffer, 1971) have also been proposed. It should be noted that Buddhue's values were derived from meteorites which not only survived atmospheric stresses but also remained intact after impact with the surface. These values, therefore, should be considered as maximum crushing strengths for the original nonfragmented meteoroids.

The altitude at which breakup occurs is a function of the strength and velocity of the meteoroid as well as of the local air density (refer to Fig. 8). The stagnation pressure, P, behind the bow shock is:

$$P = \rho_a V^2. \tag{13}$$

This pressure is exerted on the leading edge of the meteoroid. The pressure in the mete-

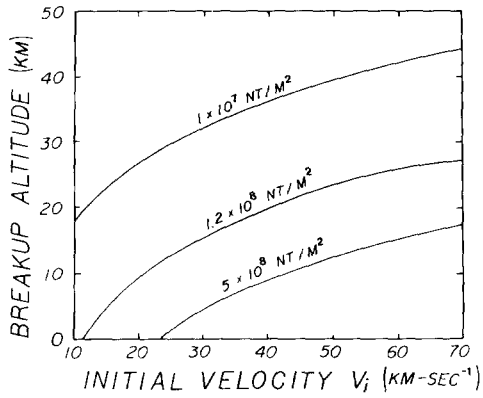

FIG. 8. Diagram showing how the breakup altitude varies for different yield strengths and velocities. This figure covers meteoroids whose masses range from 10^7 to 10^9 kg and the effects of atmospheric drag are included. It should be noted that the incoming bodies being considered are large enough that maximum deceleration is not reached before breakup (or impact) occurs.

oroid wake is nearly zero. This difference in pressure between the front and back of the meteoroid is responsible for both decelerating and crushing it. This model for breakup is essentially the same as was proposed by Baldwin and Sheaffer (1971). Krinov (1966) considers the fragmentation zone for most meteoroids to be between 12 and 30 km altitude.

Approximate breakup strengths can also be calculated using the velocities and altitudes for the breakup of observed meteoroids. The Sikhote-Alin meteoroid is said to have fragmented at an altitude of approximately 6 km with a velocity of about 14 km sec^{-1} (Fesenkov, 1951; Krinov, 1966). This gives a breakup strength of about 10^8 N m^{-2}. The Paragould meteorite (Nelson, 1953) broke up at about 16 km altitude with a velocity of 15 km sec^{-1} which gives a yield strength of 3×10^7 N m^{-2}. Other values considerably less than these are also possibilities, as would be expected in the case of "dust balls" or highly fractured meteoroids.

For the numerical modeling of the breakup of a meteoroid, yield strengths of near zero (corresponding to a breakup above 70 km), 1×10^7, 1.2×10^8, and 5×10^8 N m^{-2} were used.

Also, since the known crater fields display a range in crater sizes, the computer model meteoroid was "broken down" into different sized fragments; each fragment being one-half the mass of the next larger fragment. The individual trajectories of the fragments were then calculated by numerically integrating Eqs. 1–9 using a Runge-Kutta routine. The computation was terminated when the last fragment struck the ground and the separations between the meteorite impacts were calculated as well as the diameters of the craters formed.

CROSS-RANGE DISPERSION

All of the known crater fields exhibit a cross-range spread as well as a downrange spread (refer to Table VIII). To explain this cross-range spread, there must exist a transverse horizontal velocity component associated with the trajectory of the meteoroid fragments.

Several mechanisms for supplying a transverse velocity component to the meteoroid fragments include: the effect of transverse lift, centripetal separation from a rotating meteoroid, dynamical transverse separation resulting from the crushing breakup of the meteoroid, and the interaction of two or more bow shocks of the fragments just after breakup. Each of these are discussed in the text that follows.

Effect of Lift

The simplifying assumption of a spherical or tumbling meteoroid with zero lift may not be entirely correct and a lift perpendicular to the line of flight may play a role in the final distribution of craters.

There is a maximum value that the lift coefficient (C_L) can have for which the largest crater in a given strewn field is located at the downrange end. Values of C_L larger than this maximum value would result in a strewn field where the smallest fragments are found scattered around (and,

TABLE VIII

DIMENSIONS OF TERRESTRIAL CRATERFIELDS

Crater field	Downrange length (km)	Maximum cross-range width (km)	Ratio of reported crater diameters
Campo del Cielo	20	4	5:1
Clearwater Lakes	31	NA[a]	1.2:1
Henbury	0.64	0.44	21:1
Herault	7.3	1.8	13:1
Kaalijarv	1.0	0.75	24:1
Lonar	1.3	NA	6:1
Mauritanian craters	600	NA	5:1
Morasko	0.5	0.5	7:1
Odessa	0.2	0.09	28:1
Sikhote-Alin	2.0	0.9	265:1
Wabar	0.5	0.1	6:1

[a] Not applicable for crater fields with only two or three craters.

in particular, downrange from) the largest fragments, a pattern which is not generally found in the known crater fields.

One method for determining an approximate value for C_L is to determine the value for which the upward forces on the meteoroid during entry equal the downward forces (refer to Fig. 7 and Eq. 3). In this case, the trajectories show no steepening in their angle with respect to the horizontal as the meteoroid is decelerated by drag, and all of the fragments impact at the same downrange distance (i.e., no separate craters are produced). By this method it was found that $C_L \lesssim 10^{-3}$ and that lift cannot play an important role in the formation of terrestrial crater fields. Proof of the negligibility of lift follows.

Since more than 90% of the effective lift occurs below 20 km altitude, the average atmospheric density ($\bar{\rho}_a$) for this zone is

$$\bar{\rho}_a \simeq 0.35\ \rho_0 \tag{14}$$

then, setting $d\theta/dt = 0$ and solving for C_L (from (Eq. (3)) we see that

$$C_L \cong 2Mg \cos\theta/\bar{\rho}_a AV^2. \tag{15}$$

For meteoroid masses (M) ranging between 10^7 and 10^9 kg, and trajectory angles (θ) between 15 and 45° with respect to the horizontal, values for C_L, by this method, range from 10^{-3} to 10^{-2}.

Numerical modeling was also used to determine the maximum value for C_L. It was found that a lift coefficient (C_L) greater than about 10^{-3} would produce a crater field where some of the smaller fragments impact downrange from the larger fragments (assuming the lift to be directed transversely upward to the trajectory). Therefore, a maximum value for the lift coefficient is of order 10^{-3}.

Applying this value ($C_L = 10^{-3}$) to try and explain the cross-range spread observed in crater fields, we see

$$\alpha = \frac{F}{M} = \frac{1}{2}\frac{C_L\rho_a AV^2}{M}, \tag{16}$$

where α is acceleration and F is force and

$$Y = \frac{1}{2}\alpha t^2 = \frac{1}{4}\frac{C_L\rho_a AV^2t^2}{M}, \tag{17}$$

where Y is $\frac{1}{2}$ the cross-range separation and t is the time of flight after breakup occurs at altitude Z.

Substituting Eq. (7) for A (assuming an

iron meteoroid) and since

$$(V)(t) = Z/\sin\theta,$$

then

$$Y \simeq \frac{8 \times 10^{-7}\bar{\rho}_a Z^2}{(M)^{1/3}\sin^2\theta}. \quad (18)$$

Substituting the average value of the atmospheric density below 20 km (Eq. (14)) and letting Z equal 20 km

$$Y \simeq \frac{1.3 \times 10^2}{(M)^{1/3}\sin^2\theta}\ \text{m kg}^{1/3} \quad (19)$$

Therefore, the calculated deviation (Y) from the initial trajectory of a meteoroid (i.e., one-half the cross-range spread expected) is about 2 km for a 1-kg meteoroid and is less than 10 m for a 10^7-kg meteoroid (assuming θ is 15°). Lift, therefore, cannot account for the much larger cross-range spreads observed in known crater fields and is a relatively insignificant effect except in the case of meteoroids whose masses are less than 100 kg or for extremely shallow entry angles. Other mechanisms must, therefore, be responsible for the cross-range spreads observed in terrestrial crater fields.

Effect of Bow Shock Interaction

Immediately after fragmentation, the meteoroid fragments travel as a unit within a single bow shock. Soon afterwards the fragments become sufficiently separated that they have individual bow shocks. High pressures develop between these bow shocks, producing an acceleration transverse to the trajectory of the incoming meteoroid (refer to Fig. 9).

To calculate the value of this acceleration, assume that the bow shocks exert a force on each other until the two meteoroid fragments have a separation (β) of a certain number (C) of meteoroid radii (R_1)

$$\beta = CR_1. \quad (20)$$

Therefore, the time of interaction (Δt) is

$$\Delta t = \left(\frac{2\beta}{\alpha}\right)^{1/2}, \quad (21)$$

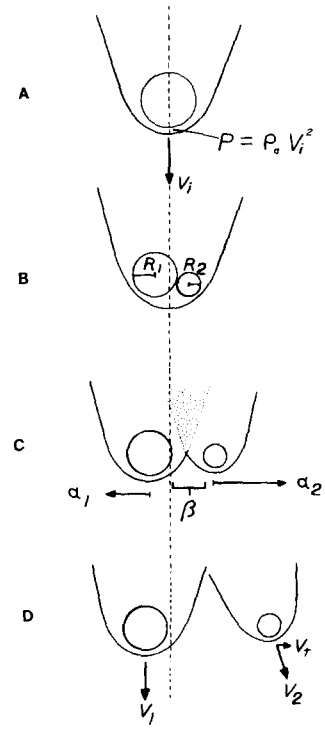

FIG. 9. Schematic diagram of how the interaction of bow shocks can produce a transverse velocity component in the trajectories after breakup. (A) Prebreakup meteoroid and trajectory with pressure building up behind the bow shock; (B) immediately after fragmentation the fragments travel as a unit with one bow shock; (C) the interaction of bow shocks produce a transverse acceleration in the fragments until they are separated by distance β; (D) finally, the interaction of the bow shocks and the transverse acceleration cease, leaving the fragments to travel in their modified trajectories (V_1 and V_2).

where α is the acceleration. The final transverse velocity V_T is

$$V_T = \alpha\Delta t = (2\beta\alpha)^{1/2}. \quad (22)$$

Recalling that

$$\alpha = \frac{F}{M} = \frac{\rho_a V_i^2 \pi R_2^2}{(4/3)\pi R_2^3 \rho_m} = \frac{3V_i^2\rho_a}{4R_2\rho_m}, \quad (23)$$

where V_i is the velocity along the trajectory and substituting Eq. (23) into Eq. (22)

$$V_T = \left(\frac{3}{2}C\frac{R_1}{R_2}\frac{\rho_a}{\rho_m}\right)^{1/2} V_i, \quad (24)$$

and since the remaining flight time (t) is

$$t = Z/V_2 \sin \theta, \tag{25}$$

where V_2 is resultant velocity along the modified trajectory, and assuming $V_2 \approx V_i$, the separation distance (Y) is

$$Y = V_T t = \left(\frac{3R_1 C\rho_a}{2R_2\rho_m}\right)^{1/2} \frac{Z}{\sin \theta}. \tag{26}$$

The maximum separation (Y_{max}) is achieved when breakup occurs at an altitude of two scale heights (about 15 km). By studying the cross-range spread of craters in known crater fields, it is possible to determine an approximate value of the constant C in Eq. (20). Using the information in Table VIII, the range in cross-range spreads is from 0.1 to about 2.0 km. From Eq. (26), the constant C is calculated to be between 0.02 and 1.52 (assuming that the ratio of crater sizes is linearly proportional to the diameters of the corresponding impacting meteorites, and assuming a 15° angle with a breakup at 15 km altitude). Since the crater fields used in this calculation are not necessarily the result of a breakup at 15 km, it should be noted that the higher value of 1.52 is more likely the true value (i.e., since breakup was assumed to occur at 15 km altitude, where the maximum separation for this mechanism occurs, an actual breakup at either higher or lower than 15 km altitude would result in a calculation of C that is lower than the true value). For this reason a value of unity is assigned to C and is probably correct to within a factor of 2.

Assuming a ratio of meteoroid radii of 1 : 6 (corresponding to the ratio of observed crater diameters in several crater fields) and using a 15° angle trajectory with a breakup at 15 km altitude, the expected cross-range spread (Y) is about 1 km (refer to Eq. (26)). This value is comparable to the cross-range spreads in Table VIII and is independent of the masses of the meteoroid fragments.

The interaction of bow shocks can result in a crater field where smaller craters are scattered completely around the main crater. A symmetric distribution of fragments around the main crater would be expected for the case of vertical entry. For entry angles less than approximately 30°, however, the separation between fragments is dominated by drag and gravity forces and essentially all of the smaller meteoroid fragments fall short of the largest fragment. The interaction of bow shocks is, therefore, primarily responsible for the cross-range spread observed, in the case of shallow angle trajectories, rather than the gravity dominated downrange spread. Lift is probably insignificant in explaining cross-range spread except in the case of fragments whose masses are less than 10^2 kg. The bow shock interaction may also be related to the explosive effect that observers describe when a meteoroid fragments (Krinov, 1966).

Effect of a Spinning Meteoroid

If one assumes that a large meteoroid is spinning at the time breakup occurs, fragments may separate from the parent body with tangential velocities sufficient to explain the cross-range separation observed in terrestrial crater fields. This, however, assumes that the spin axis of the body is oriented such that the tangential velocities of the fragments are horizontally transverse to the original initial trajectory.

Assuming that a large meteoroid enters the atmosphere at 10 km sec^{-1} with an entry angle of 15° with respect to the horizontal and that breakup occurs at 15 km altitude, a transverse velocity of about 200 m sec^{-1} is required to explain the cross-range spread observed. It can be easily shown that for a spherical meteoroid whose mass is 10^6 kg, 10 rps is required to supply this tangential velocity. For a 10^{10}-kg body, about 0.5 rps is required. The required angular velocity varies inversely with altitude of breakup and linearly with the initial velocity.

Separation Due to Crushing

Calculation of the transverse accelerations experienced by fragments as the ini-

tial body is being crushed, show that the resulting transverse velocities for large fragments may be sufficient to explain the cross-range dispersions observed in crater fields.

The separations resulting from this mechanism are roughly the same order of magnitude as the separations from bow shock interactions but are about three orders of magnitude greater than the separation due entirely to lift.

Shallow Angle Trajectories

The most probable angle of meteorite impact with a nongravitating body is 45° (Gilbert, 1893). Shoemaker (1962) extended this calculation to a gravitating body and derived the same angle, assuming no atmospheric deceleration. The probability for impact at angles less than 30° with respect to the horizontal is one of every four events. Three of every 100 events occur at angles less than 10° (Gault and Wedekind, 1978).

This paper is concerned with shallow angle entries less than about 30° because for angles steeper than 30°, there is no significant gravity separation of different mass fragments, and the separation of craters for a 45° angle trajectory would be less than 300 m if it is entirely due to the interaction of bow shocks for a ratio of meteoroid radii of 1 : 6. For an initial mass of 10^9 kg at a 45° angle, a single crater would be formed even if breakup occurs because the separation of the fragments would be insufficient to produce multiple craters. Sometimes the trajectory of an incoming meteoroid is too shallow to hit the surface. The daytime fireball of August 10, 1972 (*Sky & Tel.* 1972; Rawcliff *et al.*, 1974; Jacchia, 1974) was an example of one such meteoroid. The mass of this body has been estimated to have been 10^6 kg and its velocity was about 15 km sec^{-1}. Its entry angle was approximately 4° and the lowest point in its trajectory was at an altitude of 60 km.

There is also the possibility that a meteoroid can lose enough momentum in a shallow angle entry to become locked into a decaying geocentric orbit (assuming that impact did not occur on the first encounter). This event is unlikely unless the initial geocentric velocity is between 11.2 and 20 km sec^{-1} so that upon passage through the atmosphere, the meteoroid's velocity drops below the escape velocity.

Shallow angle entry allows for a much greater gravitational separation than normally occurs at steeper angles. Figure 10 shows the maximum separation by gravitational and drag forces that can occur between two meteoroids with masses of 10^9 and 10^8 kg for various entry angles and velocities. These two masses were chosen because at angles less than 30° a crater of order 10^2-m diameter and one about half that size would result, which correspond to the diameters encountered in terrestrial crater fields. It is interesting to note that for velocities greater than about 20 km sec^{-1}, the maximum separation between these bodies due to gravity and drag is less than 20 km, and would be less for larger objects. This, therefore, gives an upper limit for the length of a probable crater field, for similar-sized bodies with velocities greater than 20 km sec^{-1}. For initial velocities between 11.2 and 20 km sec^{-1} the separation can be very large (greater than 100 km) assuming the entry angle was less than 5° (see Fig. 10). Other effects of shallow entry include the elongation of craters, characteristic ejecta patterns and richochetting (Gault and Wedekind, 1978; Fudali and Chapman, 1975).

Comparison of Model with Known Crater Fields

Discussion

A model for meteoroid breakup and for the formation of crater fields has been presented. Figures 11, 12, and 13 show the regions of expected crater field formation for various initial masses, velocities, entry angles, and strengths of meteoroids.

Single craters are produced when either breakup has not occurred or where the

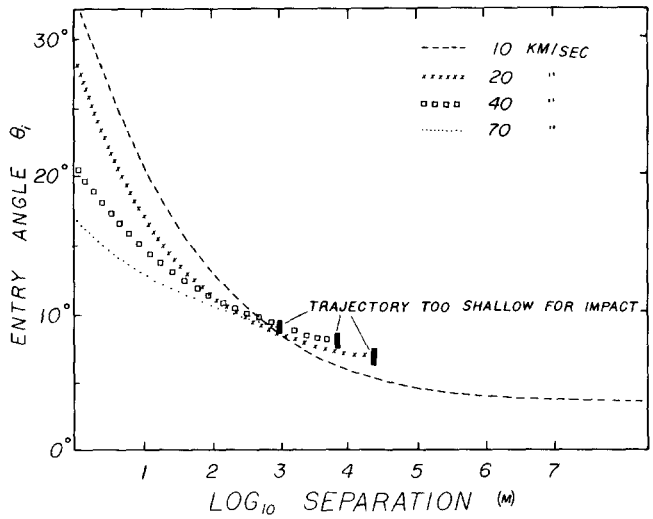

FIG. 10. Graph showing the maximum separation between two meteoroids with masses of 10^9 and 10^8 kg, respectively, as a function of velocity and entry angle. Separation was assumed to have occurred above 70 km altitude. The separation presented here is only due to the effect of gravity on the differentially decelerated meteoroids.

largest crater in a given field has a diameter larger than the separations achieved by the fragments. The region of "total overlap" is where the separation between the largest fragments is of the same order of magnitude as the diameters of the fragments themselves. The region of "some overlap" is where the largest fragments produce craters with diameters larger than their respective separations, but where the smallest craters produced are not overlapping. In the region of "no overlap," the diameters of the craters produced are much smaller than the separations between fragments. There also exists a region for which the meteoroid does not survive atmospheric ablation.

The regions shown are derived from numerical modeling of the breakup and trajectory of a meteoroid. Gravity, drag, and bow shock interaction forces are included in the computations. The effect due to a spinning parent body is roughly comparable to that due to bow shock interaction.

Figure 11 shows these zones for an entry angle of 30° and a breakup strength of 5×10^8 N m^{-2} (refer to Fig. 8 for the altitude of breakup for the various velocities). For this case, total overlap of craters occurs when the largest crater in the field is approximately 400 m in diameter. The dotted lines represent the diameter (in meters) of a crater produced by a fragment with an initial mass of one-half the mass of the meteoroid at the time of breakup. This, then, can only be used as a guide for the approximate diameter of the largest crater in a given crater field. Baldwin and Sheaffer (1971) conclude from their investigation that objects of mass less than 10^8 kg with initial velocities of 70 km sec^{-1} will not survive ablation. The much smaller surviving masses indicated on this figure may be due to the choice of C_H, the effects of breakup, or to the lower entry angle used here.

Figure 12 shows the zones for an entry angle of 15° and a breakup strength of 5×10^8 N m^{-2}. Here, due to the longer atmospheric ablation time, the crater diameters are smaller than shown on Fig. 11 for meteoroids of the same initial masses and velocities. The effect of shallower impact angles is also taken into account for the crater diameters shown.

Figure 13 shows the predicted zones for

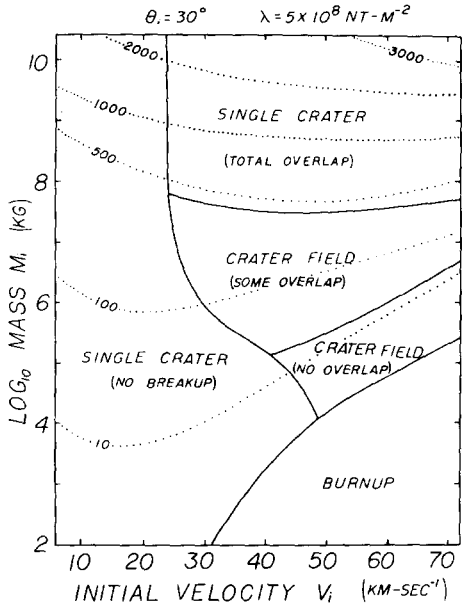

FIG. 11. Diagram showing the zones of crater field formation or burnup for meteoroids with a yield strength (λ) of 5×10^8 N m^{-2} and an entry angle (θ_i) of 30° with respect to the horizontal. The dotted contours indicate the diameter (in meters) of a crater produced by a fragment with an initial mass of one-half the mass of the meteoroid at the time of breakup. This should only be used as a guide for the approximate diameter of the largest crater in a given crater field.

an entry angle of 15° and a breakup strength of 1×10^7 N m^{-2}. Although Fig. 8 shows that for this strength, breakup would occur for any initial velocity between 10 and 70 km sec^{-1}, the small zone of no breakup (10^2–10^5 kg and 10–20 km sec^{-1}) occurs because these relatively small masses are decelerated below the velocity needed for breakup to occur at lower altitudes.

The largest crater in a strewn field is predicted to have a diameter between 100 and 1000 m and this is comparable with the largest craters in terrestrial crater fields.

The largest uncertainty in the numerical modeling is in the altitude of breakup, which is related to the yield strength of the meteoroid. Since the cross-range width of a given crater field depends primarily upon the breakup altitude and the downrange length is related to the angle of entry, it is possible to approximately derive these parameters from the terrestrial crater fields (refer to Table VIII).

Figure 14 shows a distance vs log diameter plot for terrestrial and computer-generated crater fields. The lines for the terrestrial crater fields (Fig. 14A) represent a least-squares fit of the log diameter vs the center-to-center distance from the largest crater in that crater field.

In the following estimates of entry angle and altitude of breakup for the known crater fields, the initial velocities were assumed to be between 11.2 and 30 km sec^{-1}.

Interpretation of Terrestrial Crater Field

Campo del Cielo

The extreme relative dimensions of this crater field of 20 × 4 km suggests that the entry angle was initially less than 10° and that breakup occurred at least as high as 15 km altitude. Renard and Cassidy (1971) have suggested that breakup occurred at 46 km. This possibility requires that the initial entry angle was less than about 6° to pro-

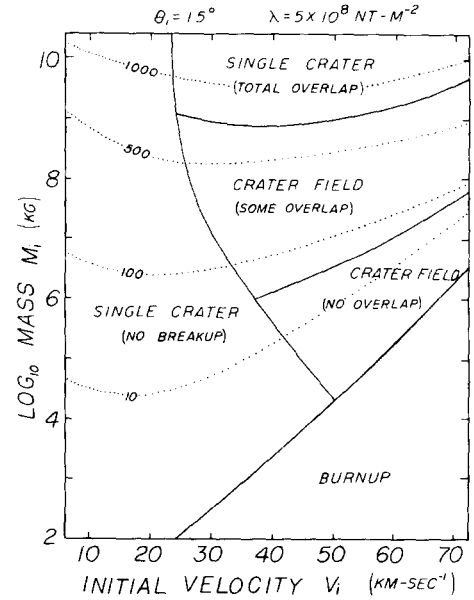

FIG. 12. Same as Fig. 11 but for an entry angle (θ_i) of 15°.

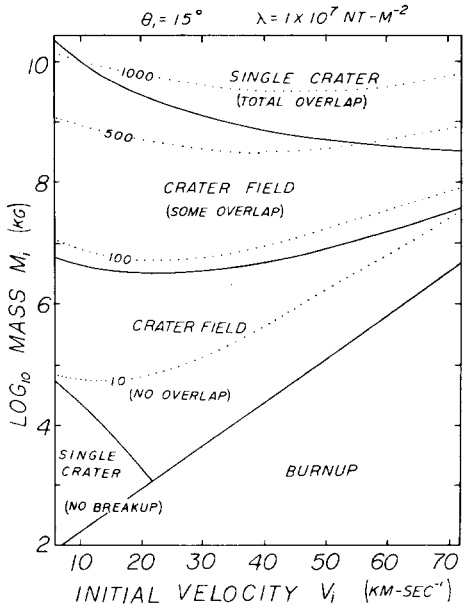

FIG. 13. Same as Fig. 11 but for a yield strength (λ) of 1×10^7 N m^{-2} and an entry angle (θ_i) of 15°.

duce the observed cross-range spread for the range of crater sizes found here.

Clearwater Lakes

Atmospheric deceleration, gravity, lift, bow shock interaction, spinning, and dynamical separation due to crushing cannot explain the large separation for craters of these sizes. A possible explanation for these craters is that they represent the impacts of binary asteroids (Binzel and Van Flandern, 1979; Tedesco, 1979).

Henbury

The dimensions of this crater field of 0.6 × 0.4 km suggest a possible breakup altitude of about 10 km with an entry angle of from 10 to 20°, depending on the velocity. Many other possibilities exist and this is only an example.

Herault

If these craters are of impact origin, they could have resulted from a low angle entry (less than 10°) with a breakup at or above 15 km altitude.

Kaalijarv

Craters 2 and 4 (refer to Figs. 3 and 15 and Table IV) appear to be too far from the main crater for their diameters, when compared with the rest of the craters in this strewn field. One possible explanation for this is if there were two stages of fragmentation resulting in two separate distance–diameter correlations as shown in Fig. 15; one occurring at a high altitude (possibly 45 km) resulting in the formation of craters 2 and 4, the other breakup occurring at about 15 km, assuming a 10 to 20° entry angle.

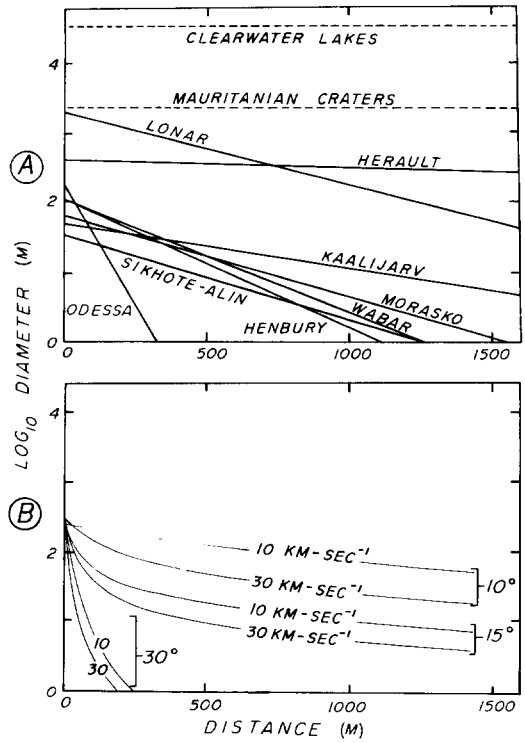

FIG. 14. (A) Graph showing a least-squares fit for log crater diameter vs center-to-center distance from the largest crater in the respective terrestrial crater fields. The line for Sikhote-Alin is the upper boundary line as shown in Fig. 16 and is not a least-squares fit for all of the craters in that crater field. (B) Graph showing calculated distributions of craters for various initial velocities and entry angles. The meteoroids were assumed to have a yield strength of 1×10^7 N m^{-2} and an initial unbroken mass of 10^8 kg. The distances shown are due to the effect of gravity on the differentially decelerated fragments.

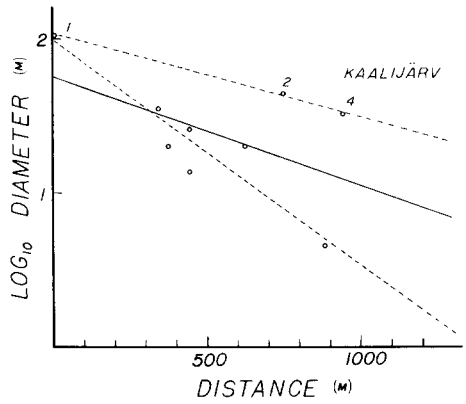

FIG. 15. Log-linear plot of crater diameter vs center-to-center distance from the largest crater in the Kaalijarv crater field. The solid line represents a least-squares fit to all of the craters. The broken lines are two separate least-squares fits indicating two possible stages of breakup with craters 2 and 4 resulting from a breakup at a much higher altitude than the rest of the craters.

Lonar Lake

The separation of the two craters of about 1300 m (center-to-center distance) cannot be explained by drag and gravity alone. However, a transverse velocity imparted by the interaction of the bow shocks for two meteoroids whose ratio of radii is 1 : 6 (assuming crater diameters scale linearly with the diameters of the impacting meteorites) yields the observed separation, assuming that the entry angle was less than 15° and that breakup occurred near 15 km. A 15° inclination is necessary to allow enough time for the observed separation and has nothing to do with the morphology of the craters.

Mauritanian Craters

The numerical modeling suggests that it is highly unlikely that these three craters are the products of the atmospheric breakup of a single large meteoroid. To achieve the observed separations of nearly 600 km, the breakup must have occurred at an altitude greater than 50 km, entry velocity was between 11.2 and 15 km sec^{-1}, and the entry angle was less than 5°.

Morasko

There is a poor correlation between the distance and crater diameters for this crater field. Also, the crater field appears to be as wide as it is long (refer to Fig. 4). This distribution of craters could be the result of an entry angle between 30 and 60° where most of the separation between craters is due to bow shock interaction rather than differential drag and gravity. A breakup altitude of between 10 and 20 km is a possibility.

Odessa

The narrow cross-range spread in this crater field of 0.09 km suggests a breakup at either below 5 or above 50 km. For a breakup below 5 km, the entry angle would be relatively shallow (10–20°), and for a breakup at about 50 km, the entry angle would be steeper (35–55°).

Sikhote-Alin

The width of this crater field is about 0.9 km and suggests a breakup occurred above 40 km for the range in crater sizes found here. To achieve the downrange spread, an initial entry angle of less than 20° is required. The impact angle has been estimated at 30° (Krinov, 1966). Krinov (1974) has identified three main stages of fragmentation of the meteoroid by studying the meteorite fragments and the overlapping scatter ellipses. He states that the first stage occurred at a high altitude, resulting in the main scatter ellipse, and was followed by two other stages as the meteoroid approached the surface, which resulted in scatter ellipses smaller than the main scatter ellipse.

The scatter of points with a definite upper boundary in Fig. 16 support the idea of a multiple breakup.

Wabar

The dimensions of this crater field can be achieved by a breakup between 10 and 30

km with an entry angle of 15 and 30° with respect to the horizontal.

CONCLUSIONS AND SUMMARY

Numerical modeling of the physics of a meteoroid trajectory and breakup in the atmosphere yields several new insights into the parameters controlling these processes. It was found that entry angles less than 30° are the most effective for the production of crater fields. Generally, the largest crater expected in any crater field should be between 100 and 750 m in diameter. For larger craters, the fragments fall so close together that the crater appears to have been made by a single unfragmented object.

Iron meteoroids with initial masses ranging from 10^5 to 10^{10} kg are the most likely to produce crater fields. The terrestrial crater fields that are discussed are probably the result of the breakup of large meteoroids whose initial masses ranged from 10^7 to 10^9 kg (with the exception of Clearwater Lakes).

The cross-range spread in known crater fields is probably produced by the interaction of bow shocks of the individual meteoroid fragments after breakup but may also be due to a combination of centripetal separation from a rotating meteoroid and a dynamical transverse separation of fragments resulting from the crushing breakup of the body. The bow shock interaction allows for a maximum cross-range separation for a breakup at approximately 15 km altitude.

A lift-to-drag ratio of 10^{-3} or less was estimated on the basis of the observed gravity-dominated separation of meteorite fragments in strewn fields. Lift is probably only important for meteoroids with masses less than 10^2 kg, or extremely shallow angles of entry (less than 8°).

The downrange spread of craters is controlled primarily by drag and gravity forces for entry angles less than 30°. For steeper angles, these forces have little effect and the separation is due to the bow shock interaction.

These considerations allow us to derive approximate values of the angle of entry and breakup altitudes form the distribution of craters in terrestrial crater fields.

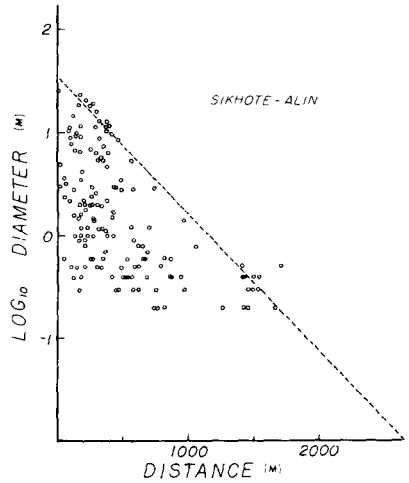

FIG. 16. Log-linear plot of crater diameter vs center-to-center distance from the largest crater in the Sikhote-Alin crater field. The scatter in the points indicates that several stages of breakup occurred. The broken line marks an approximate upper boundary for the craters and probably relates to the first stage of breakup.

ACKNOWLEDGMENTS

We would like to thank Dr. W. A. Cassidy for unpublished information relating to the Campo del Cielo crater field. Also, our appreciation is given to the anonymous reviewers for constructive comments on the original manuscript. This work was supported by NASA Grant NSG-7316.

REFERENCES

ALLEN, H. J., AND BALDWIN, B. S. (1967). Frothing as an explanation of the acceleration anomalies of cometary meteors. *J. Geophys. Res.* 72, 3483–3496.

ALLEN, H. J., AND EGGERS, J. A., JR. (1958). *A Study of the Motion and Aerodynamic Heating of Ballistic Missiles Entering the Earth's Atmosphere at High Supersonic Speeds.* NACA Report 1381.

ALLEN, H. J., AND JAMES, N. A. (1964). *Prospects for Obtaining Aerodynamic Heating Results from Analysis of Meteor Flight Data.* NASA TN D-2069.

ALLEN, H. J., SEIFF, A., AND WINOVICH, W. (1963). *Aerodynamic Heating of Conical Entry Vehicles at Speeds in Excess of Earth Parabolic Speed.* NASA TR R-185.

ALLEN, W. A., RINEHART, J. S., AND WHITE, W. C.

(1952). Phenomena associated with the flight of ultra-speed pellets, Part I. Ballistics. *J. Appl. Phys.* **23**, 132–137.

BALDWIN, B. S., AND ALLEN, H. J. (1968). *A Method for Computing Luminous Efficiencies from Meteor Data.* NASA TN D-4808.

BALDWIN, B., AND SHEAFFER, Y. (1971). Ablation and breakup of large meteoroids during atmospheric entry. *J. Geophys Res.* **76**, 4653–4668.

BALDWIN, R. B. (1963). *The Measure of the Moon.* Univ. of Chicago Press, Chicago.

BARRINGER, B. (1967). Historical notes on the Odessa meteorite crater. *Meteoritics* **3**, 161–168.

BARRINGER, R. W. (1967). World's meteorite craters ("Astroblemes"). *Meteoritics* **3**, 151–157.

BARTRUM, C. O. (1932). Meteorite craters in Arabia and Ashanti. *Brit. Astron. Assoc. J.* **42**, 398–399.

BEALS, C. S. (1964). A re-examination of the craters in the Faugères-Cabrerolles region of southern France. *Meteoritics* **2**, 85–91.

BEALS, C. S., FERGUSON, G. M., AND LANDAU, A. (1956). A search for analogies between lunar and terrestrial topography on photographs of the Canadian Shield, Part II. *Roy. Astron. Soc. Can. J.* **1**, 250–261.

BEALS, C. S., INNES, M. J. S., AND ROTTENBERG, J. A. (1960). The search for fossil meteorite craters. *Curr. Sci.* **6**, 205–262.

BINZEL, R. P., AND VAN FLANDERN, T. C. (1979). Minor planets: The discovery of minor satellites. *Science* **203**, 903–905.

BRONSHTEN, V. A. (1964). *Problems of the Movement of Large Meteoric Bodies in the Atmosphere.* NASA TT F-247.

BUDDHUE, J. D. (1942). Compressive strength of meteorites. *Pop. Astron.* **50**, 390–391.

CASSIDY, W. A. (1970). Discovery of a new multiton meteorite at Campo del Cielo (abst.). *Meteoritics* **5**, 187.

CASSIDY, W. A. (1971). A small meteorite crater: Structural details. *J. Geophys. Res.* **76**, 3896–3912.

CASSIDY, W. A., AND RENARD, M. E. (1970). On the problem of the entry trajectory of the Campo del Cielo meteorite (abst.). *Meteoritics* **5**, 187.

CASSIDY, W. A., VILLAR, L. M., BUNCH, T. E., KOHMAN, T. P., AND MILTON, D. J. (1965). Meteorites and craters of Campo del Cielo, Argentina. *Science* **149**, 1055–1064.

CHAPMAN, D. R. (1958). *An Approximate Analytical Method for Studying Entry into Planetary Atmospheres.* NACA TN 4276.

CHEN, K. K. (1975). *Study of the Ablative Effects on Tekite. Final Report* AVCO Corp., Wilmington, Mass.

CLASSEN, J. (1978). The meteorite craters of Morasko in Poland. *Meteorites* **13**, 245–255.

DENCE, M. R., GRIEVE, R. A. F., AND ROBERTSON, P. B. (1977). Terrestrial impact structures: Principal characteristics and energy considerations. In *Impact and Explosion Cratering* (D. J. Roddy, R. O. Pepin, and R. B. Merrill, Eds.), pp. 247–275. Pergamon, Oxford.

EVANS, G. L. (1961). Investigations at the Odessa meteor craters. In *Proc. Geophysical Lab./Lawrence Radiation Lab. Cratering Symposium, Washington, D.C., March 28–29, 1961.* Univ. California, Livermore, Lawrence Radiation Lab. Rept. UCRL-6438, Pt. 1, Paper D.

FESENKOV, V. G. (1951). On the motion of the sikhote-Alin meteorite. *Meteoritika* **9**, No. 3. [in Russian]

FREDRIKSSON, K., MILTON, D. J., DUBE, A., AND BALASUNDARAM, M. S. (1973). The Lonar meteorite crater, India (abst.). *Meteoritics* **8**, 35.

FUDALI, R. F., AND CASSIDY, W. A. (1972). Gravity reconnaissance at three Mauritanian craters of explosive origin. *Meteoritics* **7**, 51–70.

FUDALI, R. F., AND CHAPMAN, D. R. (1975). Impact survival conditions for very large meteorites, with special reference to the legendary Chinguetti meteorite. *Smithson. Contrib. Earth Sci.* **14**, 55–62.

FUDALI, R. F., AND CRESSY, P. J. (1976). Investigation of a new stony meteorite from Mauritania with some additional data on its find site: Aouelloul crater. *Earth Planet. Sci. Lett.* **30**, 262–268.

GAULT, D. E. (1974). Impact Cratering. In *A Primer in Lunar Geology* (R. Greeley and P. Schlitz, Eds.), NASA Ames Research Center. pp. 137–175.

GAULT, D. E., AND WEDEKIND, J. A. (1973). Diameter, depth, displaced mass, and effects of oblique trajectories for impact craters formed in crystalline rocks (abst.). *Meteoritics* **8**, 37.

GAULT, D. E., AND WEDEKIND, J. A. (1978). Experimental studies of oblique impact. In *Proc. Lunar Sci. Conf. 9th*, pp. 3843–3875. Pergamon, Oxford.

GAZLEY, C. (1961). Atmospheric entry. In *Handbook of Astronautical Engineering*, Chap. 10. McGraw-Hill, New York.

GÈZE, B., AND CAILLEUX, A. (1950). Existence probable de cratères météoriques à caberolles et à Faugeres (Herault). *C.R. Acad. Sci.* **230**, 1534–1536.

GILBERT, G. K. (1893). The Moon's face: A study of the origin of its features. *Bull. Phil. Soc. Washington* **12**, 241–292.

HAWKINS, G. S. (1964). The meteor process. In *The Physics and Astronomy of Meteors, Comets, and Meteorites.* McGraw-Hill, New York.

HEIDE, F. (1963). *Meteorites.* Univ. of Chicago Press, Chicago.

HODGE, P. W. (1965). The Henbury meteorite craters. *Smithson. Contrib. Astrophys.* **8**, 199–213.

HOFFLEIT, D. (1952). More meteor craters. *Sky & Tel.* **11**, No. 6, 134.

HOLM, D. A. (1962). New meteorite localities in the Rub' Al Khali, Saudi Arabia. *Amer. J. Sci.* **260**, 303–309.

IRWIN, J. B. (1963). Two more ancient Canadian meteorite craters. *Sky & Tel.* **26**, No. 4, 198–199.

JACCHIA, L. G. (1958). On two parameters used in the physical theory of meteors. *Smithson. Contrib. Astrophys.* **2**, 180–187.

JACCHIA, L. G. (1974). A meteorite that missed the Earth. *Sky & Tel.* **48**, No. 1, 4–9.

JACCHIA, L. G., VERNIANI, F., AND BRIGGS, R. E. (1967). An analysis of the atmospheric trajectories of 413 precisely reduced photographic meteors. *Smithson. Contrib. Astrophys.* **10**, No. 1.

JANSSEN, C. L. (1951). The meteor craters in Herault, France. *J. Roy. Astron. Soc. Can.* **45**, 190–198.

KORPIKIEWICZ, H. (1978). Meteoritic shower Morasko. *Meteoritics* **13**, 311–326.

KRANCK, S. H., AND SINCLAIR, G. W., Clearwater Lake (1963). New Quebec. *Geol. Surv. Can. Bull.* **100**, 1–25.

KRAUSS, E., MEYER, R., AND WEGENER, A. (1928). Untersuchungen über den Krater von Sall auf Ösel. *Gerlands Beitr. Geophys.* **20**, 312–378.

KRINOV, E. L. (1960). *Principles of Meteoritics* (I. Vidziunas, Transl.). Pergamon, New York.

KRINOV, E. L. (1961). The Kaalijärv meteorite craters on Saarema Island, Estonian SR. *Amer. J. Sci.* **259**, 430–440.

KRINOV, E. L. (1966). *Giant Meteorites*, (J. S. Romankiewicz, Transl.) Pergamon, New York.

KRINOV, E. L. (1974). Fragmentation of the Sikhote-Alin meteoritic body. *Meteoritics* **9**, 255–262.

LAFOND, E. C., AND DIETZ, R. S. (1964). Lonar crater, India, a meteorite crater? *Meteoritics* **2**, 111–117.

LANG, B. (1977). Thermomechanical fracturing of meteorites during atmospheric passage. In *Comets, Asteroids and Meteorites* (A. H. Delsemme, Ed.), pp. 153–157. University of Toledo, Toledo, Ohio.

MCCROSKY, R. E. (1970). Fireballs and the physical theory of meteors. *Astron. Inst. Czech. Bull.* **21**, No. 5, 271–296.

MCKINLEY, D. W. R. (1961). Physical theory of meteors. In *Meteor Science and Engineering*. McGraw-Hill, New York.

MARTIN, J. J. (1966). Kinematic motion in the atmosphere. In *Atmospheric Reentry*, Chap. 3. Prentice-Hall, Englewood, N.J.

MILLMAN, P. M. (1971). The space scars of Earth. *Nature* **232**, 161–164.

MILTON, D. J. (1963). The Campo del Cielo meteorite crater field, Argentina. *U.S. Geol. Surv. Astrogeol. Stud. Annu. Progr. Rep.*, Pt. B, 91–97 (open file report).

MILTON, D. J. (1968). *Structural Geology, Henbury Meteorite Craters, Northern Territory, Australia.* U.S. Geol. Surv. Prof. Paper 599C.

MILTON, D. J., AND DUBE, A. (1977). Ejecta at Lonar Crater, India. *Meteoritics* **12**, 311 (Abstract).

MOORE, H. J. (1976). *Missile Impact Craters, New Mexico, and Applications to Lunar Research.* U.S. Geol. Surv. Prof. Paper 812-B.

NANDY, N. C., AND DEO, V. B. (1961). Origin of the Lonar Lake and its alkalinity. *TISCO*, 144–155, July.

NELSON, H. E. (1953). *The Resistance of the Air to Stone-Dropping Meteors.* Ph.D dissertation, Augustana Library Publ. No. 24, Augustana College, Rock Island, Ill.

OPIK, E. J. (1958). *Physics of Meteor Flight in the Atmosphere.* Interscience, New York.

PHILBY, H. (1933). Rub' al Khali. *Georg. J.* **81**, 1–26.

RAWCLIFFE, R. D., BARTKY, C. D., LI, F., GORDON, E., AND AND CARTA, D. (1974). Meteor of August 10, 1972. *Nature* **247**, 449–450.

RENARD, M. L., AND CASSIDY, W. A. (1971). Entry trajectory and orbital calculations for the crater 9 meteorite, Campo del Cielo, Argentina. *J. Geophys. Res.* **76**, 7916–7923.

ROMAÑA, A., AND CASSIDY, W. A. (1973). The Campo del Cielo, Argentina meteorite crater field (abst.). *Meteoritics* **8**, 430–431.

SEIFF, A., AND TAUBER, M. E. (1966). *Minimization of the Total Heat Input for Manned vehicles Entering the Earth's Atmosphere at Hyperbolic Speeds.* NASA TR R-236.

SHOEMAKER, E. M. (1962). Interpretation of Lunar craters. In *Physics and Astronomy of the Moon* (Z. Kopal, Ed.), pp. 283–359. Academic Press, New York.

Sky & Tel. (1972). A great daylight fireball over the Northwest. *Sky & Tel.* **44**, No. 4, 269–272.

Sky & Tel. (1979). Morasko Meteorite craters, *Sky & Tel.* **57**, No. 4, 335.

TEDESCO, E. F. (1979). Binary asteroids: Evidence for their existence from light-curves. *Science* **203**, 905–907.

THOMAS, R. N., AND WHIPPLE, F. L. (1951). The physical theory of meteors. II. Astroballistic heat transfer. *Astrophys. J.* **114**, No. 3, 448–465.

VERIANI, F. (1969). Structure and fragmentation of meteoroids. *Space Sci. Rev.* **10**, 230–261.